Supporting Information for: "Using Atomic Confining Potentials for Geometry Optimization and Vibrational Frequency Calculations in Quantum-Chemical Models of Enzyme Active Sites"

Saswata Dasgupta and John M. Herbert*

Department of Chemistry and Biochemistry, The Ohio State University, Columbus, Ohio 43210 USA

January 20, 2020

*herbert@chemistry.ohio-state.edu

Table S1: Comparison vibrational frequencies for Gly-Ala. with both terminal carbons confined with potential, computed using analytic and finite-difference second derivatives.

mode	$k = 30$ N/m					$k = 450$ N/m					$k = 990$ N/m				
	freq. (cm^{-1})			error (cm^{-1}		freq. (cm^{-1})			error (cm^{-1}		freq. (cm^{-1})			error (cm^{-1}	
	analytic	IDRV=0[a]	IDRV=1[b]	IDRV=0[a]	IDRV=1[b]	analytic	IDRV=0[a]	IDRV=1[b]	IDRV=0[a]	IDRV=1[b]	analytic	IDRV=0[a]	IDRV=1[b]	IDRV=0[a]	IDRV=1[b]
1	70.12	70.12	70.08	0.00	0.04	90.49	90.48	90.52	−0.04	−0.03	84.23	84.12	84.34	0.11	−0.11
2	88.21	88.19	88.21	0.02	0.00	137.97	137.96	138.00	0.02	−0.03	95.47	95.47	95.48	0.00	−0.01
3	141.08	141.07	141.10	0.01	−0.02	182.44	182.40	182.49	0.03	−0.05	167.33	167.31	167.35	0.02	−0.02
4	264.43	264.42	264.46	0.01	−0.03	264.31	264.32	264.30	0.04	0.01	267.91	267.91	267.92	0.00	−0.01
5	285.17	285.16	285.17	0.01	0.00	311.79	311.80	311.83	0.01	−0.04	326.65	326.64	326.68	0.01	−0.03
6	291.15	291.11	291.15	0.04	0.00	332.59	332.59	332.61	0.04	−0.02	351.48	351.48	351.51	0.00	−0.03
7	326.40	326.40	326.40	0.00	0.00	395.34	395.35	395.35	0.00	−0.01	407.03	407.03	407.02	0.00	0.01
8	349.19	349.18	349.18	0.01	0.01	434.71	434.71	434.73	0.00	−0.02	492.38	492.37	492.38	0.01	0.00
9	413.53	413.53	413.55	0.00	−0.02	486.11	486.10	486.11	0.02	0.00	546.13	546.13	546.16	0.00	−0.03
10	473.06	473.05	473.08	0.01	−0.02	559.27	559.27	559.29	0.03	−0.02	617.96	617.96	617.99	0.00	−0.03
11	504.75	504.75	504.76	0.00	−0.01	574.93	574.93	574.93	0.01	0.00	659.66	659.66	659.69	0.00	−0.03
12	658.69	658.68	658.73	0.01	−0.04	658.18	658.18	658.20	0.05	−0.02	680.86	680.86	680.86	0.00	0.00
13	680.82	680.82	680.82	0.00	0.00	680.68	680.68	680.67	0.00	0.01	691.78	691.78	691.78	0.00	0.00
14	753.20	753.20	753.24	0.00	−0.04	754.44	754.44	754.44	0.04	0.00	762.07	762.07	762.06	0.00	0.01
15	790.84	790.83	790.84	0.01	0.00	790.30	790.29	790.31	0.01	−0.01	790.33	790.32	790.33	0.01	0.00
16	833.35	833.35	833.33	0.00	0.02	826.02	826.01	826.04	−0.02	−0.02	816.47	816.46	816.51	0.01	−0.04
17	851.34	851.33	851.32	0.01	0.02	840.19	840.18	840.19	−0.01	0.00	841.21	841.20	841.21	0.01	0.00
18	887.46	887.46	887.50	0.00	−0.04	892.17	892.17	892.20	0.04	−0.03	897.35	897.34	897.39	0.01	−0.04
19	905.80	905.79	905.82	0.01	−0.02	931.92	931.92	931.88	0.03	0.04	932.56	932.56	932.53	0.00	0.03
20	931.93	931.93	931.92	0.00	0.01	960.35	960.35	960.37	−0.01	−0.02	984.67	984.67	984.68	0.00	−0.01
21	959.01	959.01	959.00	0.00	0.01	1021.35	1021.35	1021.31	−0.01	0.04	1023.13	1023.13	1023.10	0.00	0.03
22	1020.34	1020.34	1020.40	0.00	−0.06	1045.70	1045.71	1045.70	0.06	0.00	1088.19	1088.19	1088.14	0.00	0.05
23	1032.95	1032.95	1032.99	0.00	−0.04	1074.23	1074.23	1074.23	0.04	0.00	1115.60	1115.60	1115.63	0.00	−0.03
24	1108.54	1108.54	1108.52	0.00	0.02	1121.64	1121.64	1121.67	−0.02	−0.03	1125.98	1125.98	1126.04	0.00	−0.06
25	1122.24	1122.24	1122.26	0.00	−0.02	1143.15	1143.15	1143.11	0.02	0.04	1151.04	1151.04	1151.12	0.00	−0.08
26	1132.38	1132.38	1132.37	0.00	0.01	1152.16	1152.16	1152.22	−0.01	−0.06	1184.79	1184.78	1184.85	0.01	−0.06
27	1152.66	1152.66	1152.69	0.00	−0.03	1160.19	1160.19	1160.22	0.03	−0.03	1209.90	1209.90	1209.89	0.00	0.01
28	1217.70	1217.70	1217.73	0.00	−0.03	1258.43	1258.43	1258.42	0.03	0.01	1272.35	1272.34	1272.33	0.01	0.02
29	1258.59	1258.60	1258.59	−0.01	0.00	1270.24	1270.24	1270.27	−0.01	−0.03	1284.52	1284.52	1284.55	0.00	−0.03
30	1276.66	1276.66	1276.64	0.00	0.02	1282.67	1282.67	1282.69	−0.02	−0.02	1297.55	1297.55	1297.48	0.00	0.07
31	1293.51	1293.51	1293.58	0.00	−0.07	1304.88	1304.88	1304.83	0.07	0.05	1337.10	1337.09	1337.04	0.01	0.06
32	1342.99	1342.98	1342.85	0.01	0.14	1343.33	1343.32	1343.23	−0.13	0.10	1376.48	1376.48	1376.44	0.00	0.04
33	1385.21	1385.21	1385.35	0.00	−0.14	1391.94	1391.94	1391.98	0.14	−0.04	1394.16	1394.16	1394.19	0.00	−0.03
34	1397.29	1397.28	1397.19	0.01	0.10	1409.73	1409.73	1409.75	−0.09	−0.02	1417.42	1417.42	1417.46	0.00	−0.04
35	1419.28	1419.28	1419.30	0.00	−0.02	1424.09	1424.08	1424.13	0.02	−0.04	1438.17	1438.16	1438.20	0.01	−0.03
36	1443.26	1443.26	1443.24	0.00	0.02	1445.70	1445.70	1445.72	−0.02	−0.02	1448.61	1448.61	1448.64	0.00	−0.03
37	1448.19	1448.19	1448.23	0.00	−0.04	1503.31	1503.30	1503.30	0.04	0.01	1505.01	1505.00	1505.00	0.01	0.01
38	1505.89	1505.89	1505.89	0.00	0.00	1525.03	1525.03	1525.06	0.00	−0.03	1525.72	1525.72	1525.74	0.00	−0.02
39	1518.97	1518.98	1518.98	−0.01	−0.01	1532.25	1532.25	1532.24	0.00	0.01	1552.08	1552.07	1552.08	0.01	0.00
40	1524.55	1524.54	1524.57	0.01	−0.02	1548.60	1548.60	1548.62	0.03	−0.02	1575.16	1575.16	1575.16	0.00	0.00
41	1531.23	1531.22	1531.23	0.01	0.00	1552.34	1552.34	1552.34	0.01	0.00	1628.56	1628.56	1628.52	0.00	0.04
42	1620.92	1620.92	1620.84	0.00	0.08	1627.09	1627.09	1627.08	−0.08	0.01	1672.22	1672.21	1672.23	0.01	−0.01
43	1699.22	1699.21	1699.23	0.01	−0.01	1698.92	1698.92	1698.95	0.02	−0.03	1703.64	1703.63	1703.65	0.01	−0.01
44	3017.93	3017.93	3017.95	0.00	−0.02	3023.10	3023.12	3023.12	0.02	−0.02	3019.32	3019.32	3019.34	0.00	−0.02
45	3033.95	3033.96	3033.97	−0.01	−0.02	3028.49	3028.50	3028.53	0.01	−0.04	3027.06	3027.05	3027.10	0.01	−0.04
46	3043.17	3043.18	3043.20	−0.01	−0.03	3035.23	3035.23	3035.24	0.02	−0.01	3037.55	3037.55	3037.56	0.00	−0.01
47	3077.55	3077.55	3077.53	0.00	0.02	3076.83	3076.84	3076.83	−0.02	0.00	3075.11	3075.11	3075.11	0.00	0.00
48	3103.11	3103.12	3103.11	−0.01	0.00	3083.44	3083.45	3083.41	−0.01	0.03	3084.11	3084.11	3084.07	0.00	0.04
49	3135.88	3135.89	3135.84	−0.01	0.04	3112.71	3112.72	3112.69	−0.05	0.02	3121.86	3121.87	3121.85	−0.01	0.01
50	3256.18	3256.18	3256.12	0.00	0.06	3251.43	3251.43	3251.44	−0.06	−0.01	3250.47	3250.47	3250.52	0.00	−0.05
51	3261.20	3261.21	3261.15	−0.01	0.05	3269.27	3269.28	3269.23	−0.06	0.04	3271.25	3271.26	3271.21	−0.01	0.04
52	3447.43	3447.44	3447.45	−0.01	−0.02	3470.88	3470.88	3470.89	0.01	−0.01	3476.45	3476.46	3476.47	−0.01	−0.02
53	3536.94	3536.94	3536.93	0.00	0.01	3574.04	3574.04	3574.02	−0.01	0.02	3581.63	3581.63	3581.61	0.00	0.02
54	3636.12	3636.14	3636.12	−0.02	0.00	3640.85	3640.86	3640.84	−0.02	0.01	3640.07	3640.08	3640.06	−0.01	0.01

[a]Second-order finite difference of energies. [b]First-order finite difference of analytic gradients.

Table S2: Anchor atoms indices for all the model systems. The anchor atoms coordinates either kept fixed (coordinate lock formalism) or constrained with a harmonic confiner

Model	Anchor atom indices																
AMDase (Model I)	3	9	17	20	23												
AMDase (Model II)	3	14	18	19	22	33	37	44	50	51	55	62	69	70	71	74	84
4-OT	17	18	22	27	28	34											

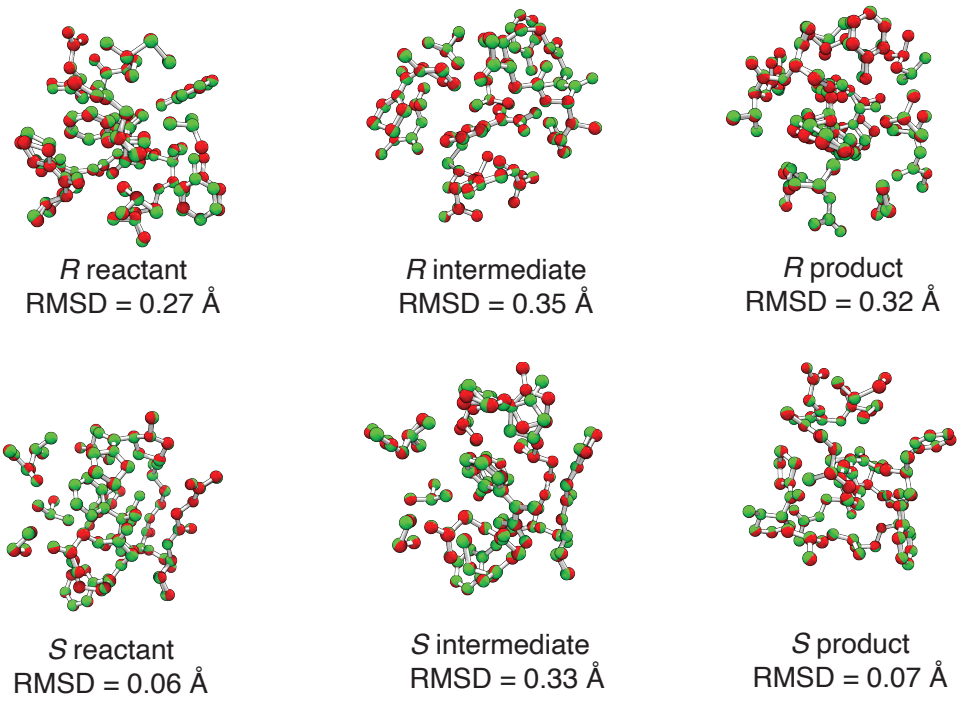

Figure S1: Optimized structures for model II of methyl(phenyl)malonate in the active site of AMDase, overlaying the structures obtained using harmonic and fixed-atom constraints.

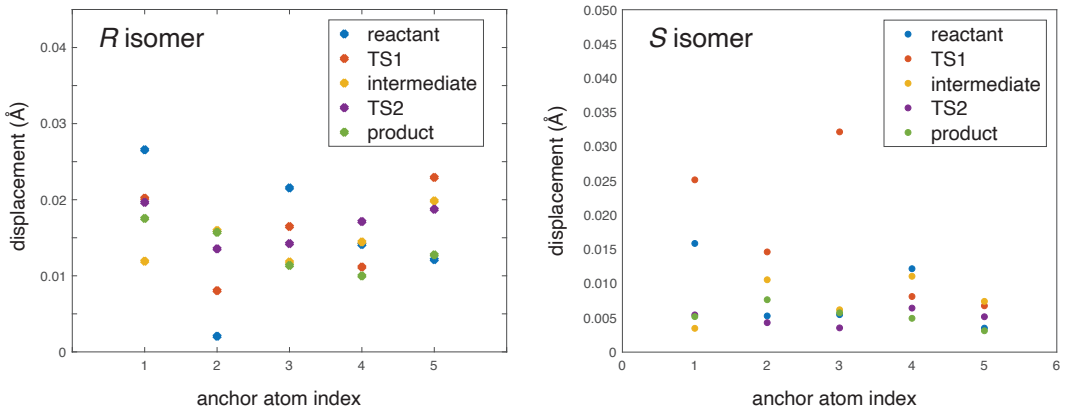

Figure S2: Displacements of the constrained "anchor atoms" as compared to their initial, crystallographic positions $\mathbf{r}_i^0$, for model I of methyl(phenyl)malonate in AMDase.

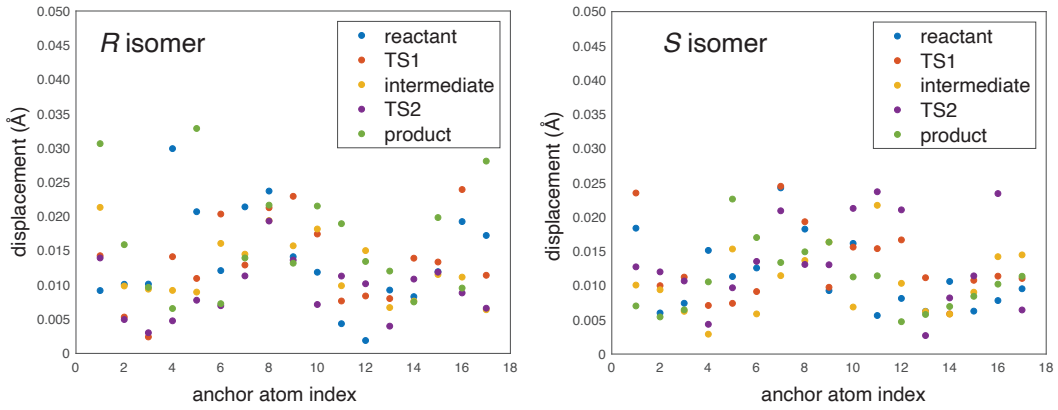

Figure S3: Displacements of the constrained "anchor atoms" as compared to their initial, crystallographic positions $\mathbf{r}_i^0$, for model II of methyl(phenyl)malonate in AMDase.

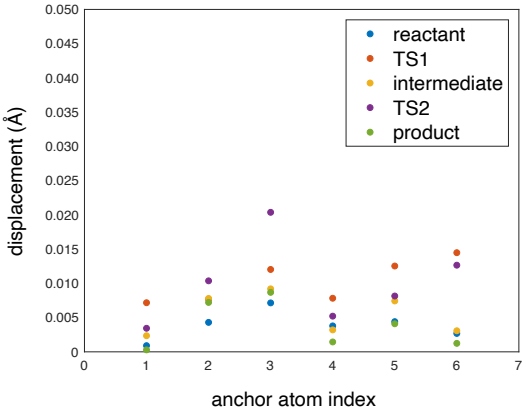

Figure S4: Displacements of the constrained "anchor atoms" as compared to their initial, crystallographic positions $\mathbf{r}_i^0$, for the reaction catalyzed by 4-OT.

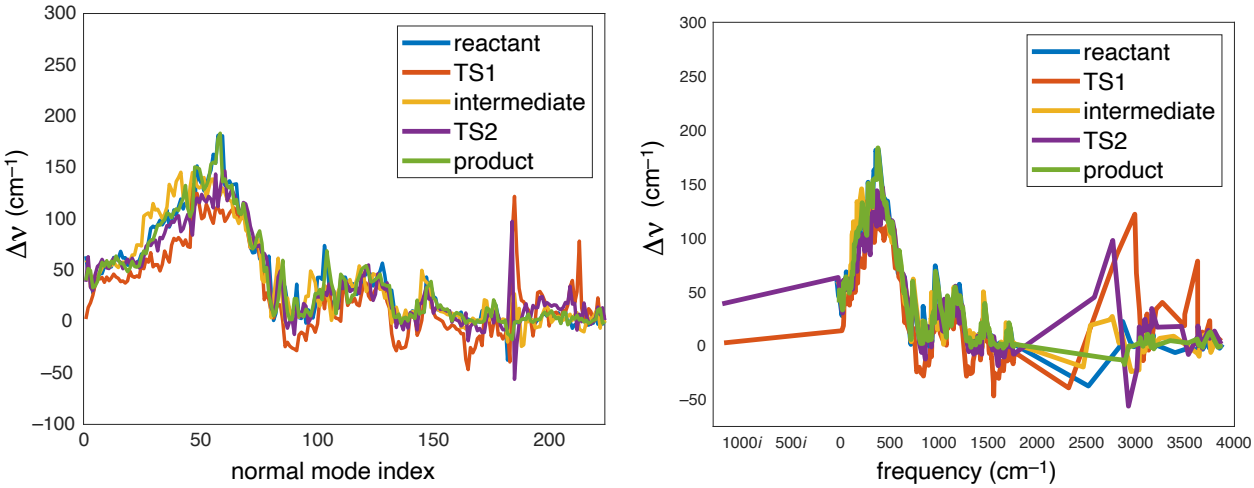

Figure S5: Differences in vibrational frequencies, $\Delta\nu = \nu$(harmonic conf.) $- \nu$(fixed atom), for each of the stationary points optimized for the 4-OT–catalyzed tautomerization of 2-oxo-4-hexenedioate. (a) Plot of $\Delta\nu$ versus the normal mode index, with the modes ordered by increasing vibrational frequency, for each stationary point along the reaction pathway. (b) Plot of $\Delta\nu$ versus the frequency ν(fixed atom).